Nuclear Instruments and Methods in Physics Research A 347 (1994) 92–97
North-Holland

NUCLEAR INSTRUMENTS & METHODS IN PHYSICS RESEARCH
Section A

Optimization of circularly-polarized radiation from an elliptical wiggler, asymmetric wiggler, or bending magnet

Chun-Xi Wang *, Ross Schlueter

The Advanced Light Source, Lawrence Berkeley Laboratory, University of California, Berkeley, CA 94720, USA

To collect circularly-polarized radiation from a bending magnet, elliptical wiggler, or asymmetric wiggler source, one must choose operating parameters to optimize their output according to user requirements. The trade-off between flux and degree of circular polarization is a basic feature of such dipole-type sources. In this paper, we discuss how to optimize the output based on two different criteria. The first is to maximize the intensity times the square of circular polarization degree (IP^2), a widely used figure of merit in circular-dichroism experiments. The second is to maximize the intensity for a given degree of circular polarization, which is desirable in some cases. The results presented here provide guidelines for the design and operation of dipole-type sources to generate circularly-polarized radiation.

1. Introduction

To satisfy the need for circularly-polarized light sources, many specially-designed insertion devices have appeared [1,2]. According to their radiation characteristics, they can be classified into wiggler/dipole-type devices and undulator-type devices. Based on the stationary phase approximation [3], radiation properties of the former type devices can be understood via a series of incoherent dipole radiation (hence we refer to them as dipole-type) sources. A common feature of dipole-type devices is the trade-off between the attainable flux density S_0 and the degree of circular polarization P_c [3,4]. These competing quantities are characterized by Stokes parameters S_0 and S_3:

$$S_0 = \langle E_x^2 + E_y^2 \rangle, \qquad S_3 = 2\,\mathrm{Im}\langle E_x E_y^* \rangle$$
$$\text{and} \qquad P_c \equiv \frac{S_3}{S_0}. \tag{1}$$

Choosing device parameters to maximize flux density while providing the required circular-polarization degree or to optimize other figures of merit in terms of experimental requirements is germane to the design and operation of such devices. Results of such optimizations are applicable for bending magnets, asymmetric wigglers, and elliptical wigglers.

Let us examine the functional form of the electric field E_x and E_y for dipole-type devices. For a bending magnet, the expressions are well known [5]:

$$\begin{aligned} E_x &= \text{const}\cdot\gamma y(1+X^2)K_{2/3}\left(y[1+X^2]^{3/2}\right) \\ &\equiv \text{const}\cdot\gamma \mathcal{E}_x, \\ E_y &= -\mathrm{i}\cdot\text{const}\cdot\gamma yX\sqrt{1+X^2}\,K_{1/3}\left(y[1+X^2]^{3/2}\right) \\ &\equiv -\mathrm{i}\cdot\text{const}\cdot\gamma \mathcal{E}_y, \end{aligned} \tag{2}$$

where

$$y \equiv \frac{E_p}{2E_c} = \frac{E_p}{1.33E_e^2B}, \qquad X = \gamma\psi,$$

$$\text{and} \qquad \text{const} = \sqrt{\frac{3\alpha}{\pi^2}\frac{\Delta\omega}{\omega}\frac{I}{e}}.$$

The const normalizes S_0 to flux density. Although there are four controllable factors: electron energy E_e or γ, magnetic field B, photon energy E_p, and vertical observation angle ψ, only two parameters y and X determine the characteristics of the radiation pattern. As long as the optimization is done in 2-D parameter space (y, X), it is clear how to choose the four controllable factors according to the above relationships. The radiation mechanism of wigglers to generate circularly-polarized light is illustrated in Fig. 1. The bottom curve represents a typical horizontal component of a trajectory, and the top three are the vertical components of the trajectories in different devices. The short bars centered on poles represent small bending-magnet sources. Neglecting the source depth effect, for an N

* Corresponding author. Present address: Applied Physics Department, Stanford University, Stanford, CA 94305-4090, USA.

SSDI 0168-9002(94)00409-Z

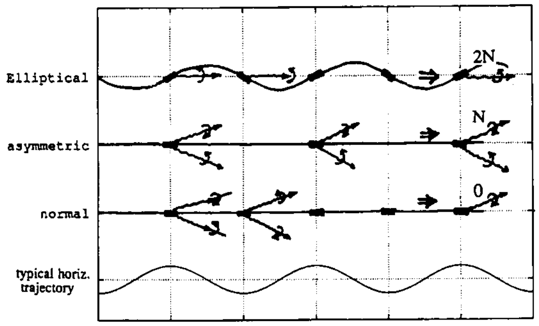

Fig. 1. Mechanism to generate elliptically polarized photons in wigglers. Not all arrows indicating radiation are shown.

period wiggler, the radiation characteristics of the asymmetric wiggler is simply N times the bending-magnet radiation (when the minor pole radiation is negligible). For the elliptical wiggler it is equivalent to N times the radiation of two bending magnets that tilt up and down respectively with respect to the orbit plane by an angle K_x/γ, where K_x is the deflection parameter of the horizontal field. For the elliptical wiggler we have an additional free parameter, K_x. However, as shown in ref. [3], the radiation of interest is the near on-axis portion, where an elliptical wiggler generating circularly-polarized photons performs best. For the on-axis case, the flux density reduces to $2N$ times of that given by Eqs. (1) and (2) but with $X = K_x$. General expressions for off-axis E_x and E_y analogous to Eq. (2) can be found in ref. [2]. Therefore, the optimization based on Eqs. (1) and (2) in (y, X) parameter space is applicable to any dipole-type device. Of course, the radiation collected is also dependent on the acceptance angle and electron beam emittance. The influence of the electron beam emittance is approximately equivalent to averaging over a finite acceptance angle. In this paper, we only consider the zero-emittance case. Usually increasing the acceptance angle will increase the flux but decrease the degree of circular polarization. Still, optimization based on flux density of a single electron should be a good indicator for the angle and emittance-included optimization, and this keeps the problem manageable. Optimization criteria are experiment dependent. In sections 2 and 3 we present optimization procedures for two reasonable criteria.

2. Optimization based on $\sqrt{I}P_c$

For a circularly-polarized light source, a common figure of merit is $\sqrt{I}P_c$, which is proportional to the signal-to-noise ratio in circular-dichroism experiments [3,6]. Thus, one would like to maximize this figure in the attainable device parameter space. I is the radiation intensity, i.e. the Stokes parameter S_0. From Eqs. (1) and (2) we have:

$$IP_c^2 = 4(\mathrm{const}\cdot\gamma)^2 \frac{E_x^2 E_y^2}{E_x^2 + E_y^2} \equiv 4(\mathrm{const}\cdot\gamma)^2 f(y, X). \tag{3}$$

The necessary condition to have an extremum is:

$$\partial f = \frac{2E_x E_y}{\left(E_x^2 + E_y^2\right)^2}\left[E_y^3 \partial E_x + E_x^3 \partial E_y\right] = 0. \tag{4}$$

More precisely, for a given X, $\partial_y f = 0$; or for a given y, $\partial_X f = 0$; or for the 2-D case, $\partial_y f = \partial_X f = 0$. Since we want to optimize the circularly-polarized radiation, neither E_x nor E_y can be zero. Thus, the part of Eq. (4) in brackets must be zero. The derivatives are:

$$\begin{aligned}
\partial_y E_x &= \tfrac{1}{3}(1+X^2)K_{2/3} - y(1+X^2)^{5/2}K_{1/3} \\
&= \frac{1}{3y}E_x - \frac{1}{X}(1+X^2)^2 E_y, \\
\partial_y E_y &= \tfrac{2}{3}X\sqrt{1+X^2}K_{1/3} - yX(1+X^2)^2 K_{2/3} \\
&= \frac{2}{3y}E_y - X(1+X^2)E_x, \\
\partial_X E_x &= -3y^2X(1+X^2)^{3/2}K_{1/3} \\
&= -3y(1+X^2)E_y, \\
\partial_X E_y &= y\sqrt{1+X^2}K_{1/3} - 3y^2X^2(1+X^2)K_{2/3} \\
&= \frac{1}{X}E_y - 3yX^2E_x,
\end{aligned} \tag{5}$$

where the following relationships between the modified Bessel functions and their derivatives are used [7]

$$\begin{aligned}
K'_{2/3}(z) &= -K_{1/3} - \frac{2}{3}\frac{1}{z}K_{2/3}, \\
K'_{1/3}(z) &= -K_{2/3} - \frac{1}{3}\frac{1}{z}K_{1/3}.
\end{aligned} \tag{6}$$

Using Eq. (5), $\partial_y f = 0$ and $\partial_X f = 0$ result in:

$$\left(\frac{E_x}{E_y}\right)^4 - \frac{2}{3yX(1+X^2)}\left(\frac{E_x}{E_y}\right)^3 - \frac{1}{3yX(1+X^2)}\left(\frac{E_x}{E_y}\right) + \frac{1}{X^2} + 1 = 0 \tag{7A}$$

and

$$\left(\frac{E_x}{E_y}\right)^4 - \frac{1}{3yX^3}\left(\frac{E_x}{E_y}\right)^3 + \frac{1}{X^2} + 1 = 0. \tag{7B}$$

Let us find the maximum in the 2D parameter space first.

In this case, the two equations of Eq. (7) are valid simultaneously. Hence, they reduce to:

$$\begin{cases} \dfrac{E_x}{E_y} = \dfrac{X}{\sqrt{1-X^2}} = \dfrac{K_{2/3}\left[y(1+X^2)^{3/2}\right]}{K_{1/3}\left[y(1+X^2)^{3/2}\right]} \cdot \dfrac{\sqrt{1+X^2}}{X} \\ y = \dfrac{X^2\sqrt{1-X^2}}{3(1-X^2-X^4+2X^6)} \end{cases}, \tag{8}$$

while

$$P_c = \frac{2E_xE_y}{E_x^2+E_y^2} = 2X\sqrt{1-X^2}$$

at this point. Eq. (8) can be solved numerically and the solution is:

$$X = 0.878, \quad y = 0.223, \quad P_c = 84\%,$$

$$S_0 = 1.4 \times 10^{10} E_e^2, \quad IP_c^2 = 1.0 \times 10^{10} E_e^2, \tag{9}$$

where E_e is in GeV, S_0 and IP_c^2 in photons/s/0.1%bw/mrad^2/mA/pole. These numbers represent the best possible performance of dipole-type devices in generating circularly-polarized radiation. Hence they are characteristic values of this type of device, and are useful for comparing the relative performance of different devices. Through Eq. (9) one can estimate optimal radiation from a particular device based on the storage ring energy and the number of effective dipoles. It is also clear that a device is most efficient at producing circularly-polarized photons of energy around $0.45E_c$.

When the parameters in Eq. (9) are not attainable, which is frequently the case, one needs to solve Eqs. (7A) and (7B) separately to find optimized values. A more concise way to attack the problem is via a contour map of various parameters of interest, such as the figure of merit, in the 2D parameter space (y, X). In Fig. 2a we show such a map of the flux density (solid line) and degree of circular polarization. The contours are in increments of 10%. The intensity contour provides a good representation of the angular and spectral characteristics of dipole radiation. With the P_c contour, the tradeoff between intensity and P_c is clear. Fig. 2b is a map of $\sqrt{I}P_c$, the figure of merit. Through this map it is clear to what extent one needs to optimize the operating parameters and what part of the energy spectrum a device can cover. Although a finite vertical acceptance angle will change these maps somewhat as shown below, they nonetheless are good guidelines to the optimization of circularly-polarized radiation in dipole-type devices. Moreover, the vertical dimension of the $\sqrt{I}P_c$ contours provides a good estimate of a suitable acceptance angle.

One noticeable feature in Fig. 2b is that, with the exception of the best performance region indicated by Eq. (9), for the same figure of merit $\sqrt{I}P_c$, one has much

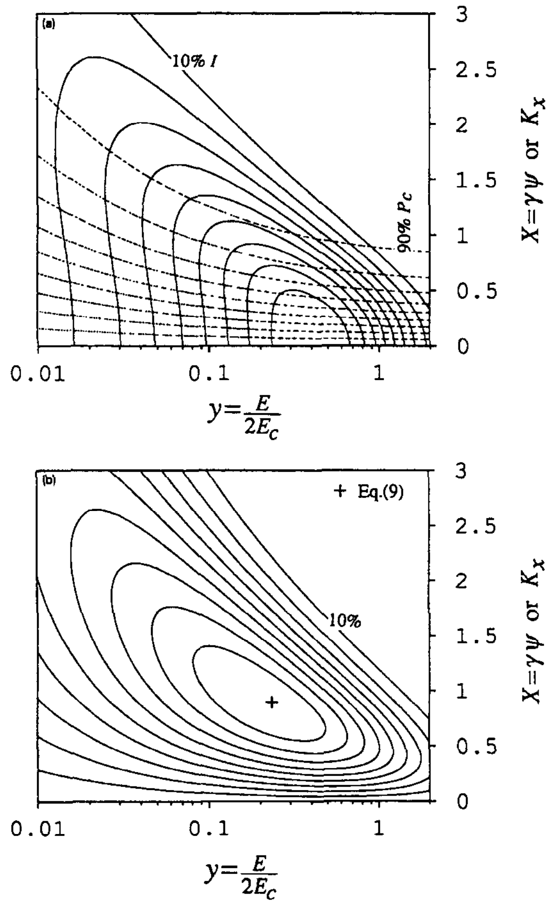

Fig. 2. (a) Contour maps of flux density and P_c; (b) contour map of $\sqrt{I}P_c$, the figure of merit.

freedom to choose various working points in parameter space with widely different intensity and polarization status. Our maps provide the information necessary for users to make their choice in favor of their particular experiments while maintaining the same signal-to-noise ratio.

Analogous to Fig. 2, Figs. 3 and 4 show the effect of acceptance angle. These maps provide an estimate of the influence of acceptable angle and beam emittance. An adjustable aperture allows experimenters to fine-tune and customize their intensity/polarization tradeoff.

3. Maximization of the flux density for a given P_c

We now present a procedure to optimize the circularly-polarized radiation according to a different criterion: maximization of the flux density for a given P_c. As shown in Fig. 2a, along the contour lines of P_c, the flux density changes rapidly. Our purpose here is to calculate the flux density along these constant P_c curves and find the maxim. Expressed mathematically, we maximize the function

$g(y, X) = S_0$ under the constraint $\phi = \phi(y, X) \equiv S_3 - P_c S_0 = 0$. This can be solved by the standard Lagrange multipliers method as follows. Define the Lagrange function with the multiplier λ as $L(y, X, \lambda) = S_0 + \lambda\phi$, the necessary conditions to reach extremum of $g(y, X)$ are:

$$\begin{cases} \dfrac{\partial L}{\partial y} = 2\left\{\left[(1-\lambda P_c)E_x + \lambda E_y\right]\partial_y E_x \right. \\ \qquad \left. + \left[(1-\lambda P_c)E_y + \lambda E_x\right]\partial_y E_y\right\} = 0 \\ \dfrac{\partial L}{\partial X} = 2\left\{\left[(1-\lambda P_c)E_x + \lambda E_y\right]\partial_X E_x \right. \\ \qquad \left. + \left[(1-\lambda P_c)E_y + \lambda E_x\right]\partial_X E_y\right\} = 0 \\ \dfrac{\partial L}{\partial \lambda} = S_3 - P_c S_0 = -P_c\left\{E_x^2 + E_y^2 - \dfrac{2}{P_c}E_x E_y\right\} = 0. \end{cases} \tag{10}$$

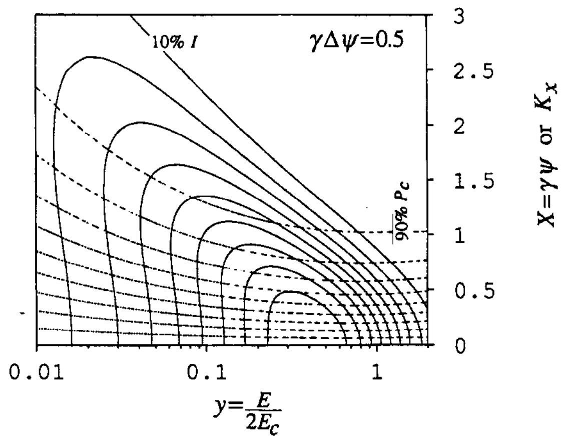

Contour map of $\sqrt{I}\,P_C$, the figure of merit

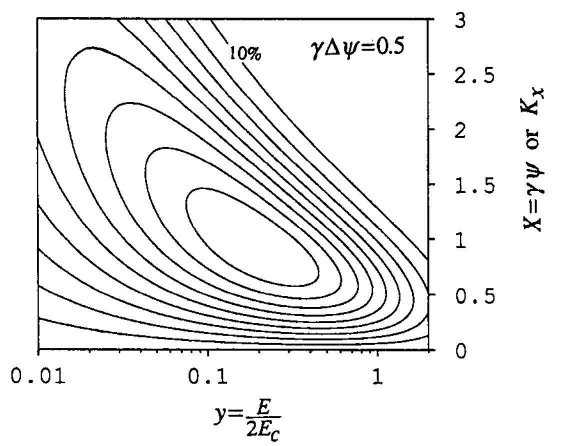

Fig. 3. Contour maps of flux, P_c, and $\sqrt{I}P_c$ with vertical acceptance angle $\gamma\Delta\psi = 0.5$.

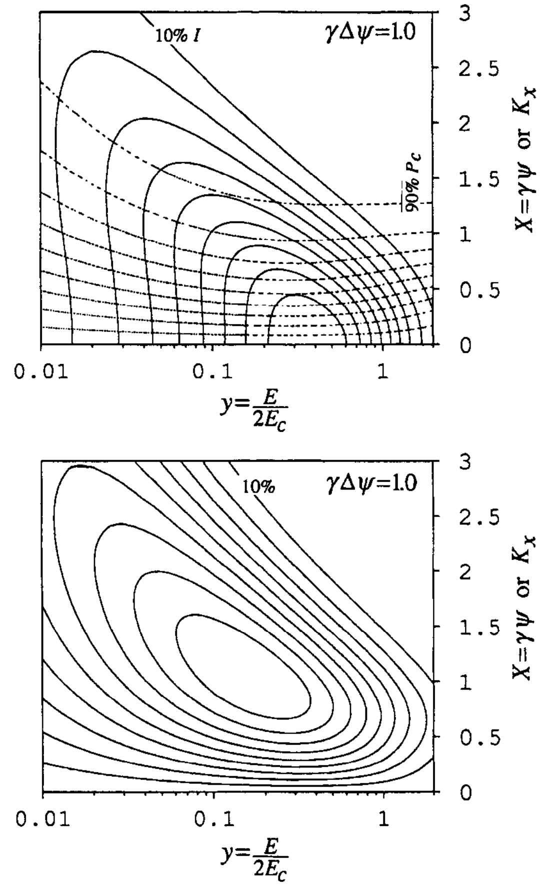

Fig. 4. Contour maps of flux, P_c, and $\sqrt{I}P_c$ with vertical acceptance angle $\gamma\Delta\psi = 1.0$.

In general, $[(1-\lambda P_c)E_x + \lambda E_y][(1-\lambda P_c)E_y + \lambda E_x] \neq 0$, so Eq. (10) reduces to:

$$\begin{cases} \partial_y E_x \partial_X E_y = \partial_y E_y \partial_X E_x \\ E_x^2 + E_y^2 - \dfrac{2}{P_c}E_x E_y = 0. \end{cases} \tag{11}$$

Using Eq. (5), Eq. (11) becomes:

$$\begin{cases} \left(\dfrac{E_x}{E_y}\right)^2 - 2\dfrac{1}{6yX^3}\left(\dfrac{E_x}{E_y}\right) + \dfrac{1-X^4}{X^4} = 0 \\ \left(\dfrac{E_x}{E_y}\right)^2 - 2\dfrac{1}{P_c}\left(\dfrac{E_x}{E_y}\right) + 1 = 0. \end{cases} \tag{12}$$

From Eq. (12), holding P_c constant, S_0 reaches its extremum at the values of X and y given by the solution of the simultaneous equations:

$$\begin{cases} \frac{1}{3yX^3} = \frac{1}{X^4 P_c} \pm \sqrt{\left(\frac{1}{X^4} - 2\right)^2 \left(\frac{1}{P_c^2} - 1\right)} \\ \frac{E_x}{E_y} = \frac{1}{P_c} \pm \sqrt{\frac{1}{P_c^2} - 1} \\ - = \frac{\sqrt{1+X^2}}{X} \frac{K_{2/3}\left(y[1+X^2]^{3/2}\right)}{K_{1/3}\left(y[1+X^2]^{3/2}\right)}. \end{cases} \quad (13)$$

We solve these equations numerically. Their solutions over the polarization range $0.5 \leq P_c < 1.0$ are tabulated in Table 1 along with the flux density (normalized to one pole and with $E_e = 1$ GeV, as in Eq. (9)) and $\sqrt{I} P_c$. The significance of this table is equivalent to Eq. (9) but with a different criterion. It shows the best tradeoff between P_c and maximum possible flux density. Of course, the performance listed in this table is attained only if the corresponding X and y are realizable, which may not always be the case. Generally, the relationship between X and y to maintain a specific P_c is given by the second equation of Eq. (13), which is the P_c contour in Fig. 2a. The flux densities along some P_c contours are given in Fig. 5. For a practical device, only parts of (y, X) parameter space are attainable. According to Figs. 2a and 5, we can choose the attainable working point that gives maximum flux output for a given P_c.

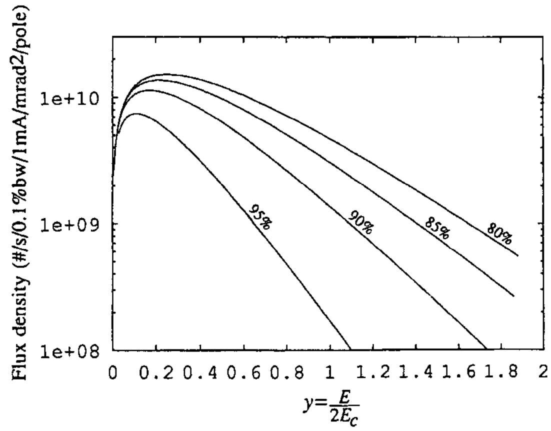

Fig. 5. Flux density vs. y for given P_c.

In Table 1, for $P_c > 90\%$ the flux drops sharply, while the corresponding X and y change rapidly as well. Thus, generally, dipole-type sources efficiently produce radiation with a degree of circular-polarization up to 90% according to the criterion used in this section. In contrast, the $\sqrt{I} P_c$ values change slowly in Table 1. From Figs. 2 (or Table 1) we see that, according to the criterion used in section 2, the dipole-type device works best for P_c between 75 and ~ 90% and is still quite good for even higher degree of circular polarization.

Table 1
Optimized intensity I for a given P_C

P_c	X	y	I	$\sqrt{I} P_c$ $(\times 10^5)$
0.500	0.353	0.366	1.86×10^{10}	0.68
0.525	0.376	0.360	1.85×10^{10}	0.71
0.550	0.401	0.352	1.84×10^{10}	0.75
0.575	0.426	0.346	1.82×10^{10}	0.78
0.600	0.453	0.339	1.80×10^{10}	0.80
0.625	0.482	0.330	1.78×10^{10}	0.83
0.650	0.512	0.322	1.76×10^{10}	0.86
0.675	0.545	0.312	1.73×10^{10}	0.89
0.700	0.581	0.302	1.70×10^{10}	0.91
0.725	0.621	0.290	1.66×10^{10}	0.93
0.750	0.664	0.279	1.62×10^{10}	0.96
0.775	0.713	0.266	1.57×10^{10}	0.97
0.800	0.769	0.250	1.52×10^{10}	0.98
0.825	0.833	0.234	1.45×10^{10}	0.99
0.850	0.912	0.213	1.37×10^{10}	0.99
0.875	1.006	0.194	1.27×10^{10}	0.98
0.900	1.128	0.172	1.14×10^{10}	0.96
0.925	1.302	0.143	9.73×10^{9}	0.91
0.950	1.580	0.109	7.44×10^{9}	0.82
0.975	2.171	0.066	4.11×10^{9}	0.63
0.990	3.290	0.032	1.34×10^{9}	0.36

4. Conclusion

In this paper, we present the optimization of circularly-polarized radiation from dipole-type devices. The universal results are applicable to bending magnets, asymmetric wigglers and elliptical wigglers of any parameters in any storage ring. Working with the intrinsic 2D (y, X) parameter space of such devices, we show optimizations according to two different criteria. The best performance under each criterion is calculated. These characteristic values are good indicators of device performance and are very useful in terms of comparison of different devices. Our results, especially the maps which give a concise representation of the radiation characteristics, are of practical importance to the design and operation of circularly-polarized radiation sources. They provide information for the device design parameter (e.g. field strength, K_x) range to cover user requirements. For individual experiments, they allow users to choose the working point in parameter space for the best tradeoff between flux and circular-polarization degree or in favor of other experimental requirements. Results presented here assume ideal sinusoidal field with negligible end effects, which requires careful attention [3]. These results are exact for small acceptance angle and zero emittance. They may change slightly for cases requiring a relatively large aperture or considering electron beam emittance.

Acknowledgments

The authors acknowledge helpful communication with C.T. Chen as well as many discussions with P. Heimann and E. Hoyer. This work was supported by the Director, Office of Energy Research, Office of Basic Energy Science, Materials Science Division of the U.S. Department of Energy, under contract No. DE-AC03-76SF00098.

References

[1] P. Elleaume, Rev. Sci. Instr. 60 (1989) 1830.
[2] H. Kitamura and S. Yamamoto, Rev. Sci. Instr. 63 (1992) 1104.
[3] C. Wang, R. Schlueter, E. Hoyer and P. Heimann, these Proceedings (8th Nat. Conf. on Synchrotron Radiation Instrumentation, Gaithersburg, MD, USA, 1993) Nucl. Instr. and Meth. A 347 (1994) 67.
[4] C.T. Chen, Rev. Sci. Instr. 63 (1992) 1229.
[5] X-ray Data Booklet, ed. D. Vaughan (Center for X-ray Optics, Lawrence Berkeley Lab., 1985) p. 4-1.
[6] C.T. Chen, private communication.
[7] Handbook of Mathematical Functions, eds. M. Abramowitz and I.A. Stegun (Dover, New York, 1971) p. 361.